



**HAL**  
open science

## Study of 6061 weld heat affected zones made with GMAW

Angélique Benoit, M. Besse, R. Louahdi, H. Paul, P. Paillard, T. Baudin

► **To cite this version:**

Angélique Benoit, M. Besse, R. Louahdi, H. Paul, P. Paillard, et al.. Study of 6061 weld heat affected zones made with GMAW. 9th International Conference on Trends in Welding Research, Jun 2012, Chicago, United States. hal-00981590

**HAL Id: hal-00981590**

**<https://hal.science/hal-00981590>**

Submitted on 30 Oct 2023

**HAL** is a multi-disciplinary open access archive for the deposit and dissemination of scientific research documents, whether they are published or not. The documents may come from teaching and research institutions in France or abroad, or from public or private research centers.

L'archive ouverte pluridisciplinaire **HAL**, est destinée au dépôt et à la diffusion de documents scientifiques de niveau recherche, publiés ou non, émanant des établissements d'enseignement et de recherche français ou étrangers, des laboratoires publics ou privés.

# Study of 6061 weld heat affected zones made with GMAW

A. Benoit<sup>1,2,3</sup>, M. Besse<sup>3</sup>, R. Louahdi<sup>3,4</sup>, H. Paul<sup>5</sup>, P. Paillard<sup>3,\*</sup>, T. Baudin<sup>1</sup>

<sup>1</sup> CNRS, UMR8182, ICMMO, Laboratoire de Physico-Chimie de l'Etat Solide, 91405 Orsay, France

<sup>2</sup> Univ Paris-Sud, 91405 Orsay, France

<sup>3</sup> LUNAM - Institut des Matériaux Jean Rouxel UMR 6502 Université de Nantes CNRS, 2 rue de la Houssinière, BP 32229, 44322 Nantes Cedex 3, France

<sup>4</sup> Institut d'Optique et de Mécanique de Précision (IOMP), Université Ferhat Abbas, Sétif Algeria

<sup>5</sup> Institute of Metallurgy and Materials Science, PAS, 30-059 Krakow, 25 Reymonta St., Poland

\*corresponding author: pascal.paillard@univ-nantes.fr

## Keywords

6061 aluminum alloy, precipitation hardening, GMAW, infrared thermography, microhardness mapping, TEM.

## Introduction

6xxx aluminum alloys are widely used in the industry for their properties such as mechanical properties, corrosion resistance, weldability or good formability. Among the 6xxx aluminum alloys, the 6061 is one of the alloys most employed for structural application [1, 2, 3] and is commonly welded. Welding is a joining operation which impairs base metal because of the high heat input used. It creates a zone where mechanical properties are different from the base metal which is called heat affected zone (HAZ). In the 6xxx aluminum alloy the HAZ is softer than base metal. Softening is due to the reversion of hardening precipitates  $\beta''$  which are heat sensitive [4]. So, the characterization of this part is critical for the design of structural parts. 6061 welding have been already studied, especially using laser welding [5, 6], arc welding [7, 8, 9] or friction welding [10, 11]. Some kinds of processes have been compared for example laser, friction stir and metal inert gas (MIG) [7] or tungsten inert gas (TIG) and laser [6]. In this study, we focus on arc welding processes. Different HAZ produced with four arc welding processes are examined. MIG and derivatives, pulsed MIG and Cold Metal Transfer (CMT®) MIG, are compared to TIG process. TIG is a reference due to its ability to produce quality weld. The processes are compared through the analysis of the HAZ. Making easier the comparison, the linear welding energy of MIG weld was similar. Regarding TIG, because the process is too different from MIG, it was not possible to use same linear welding energy. So parameters were adjusted to obtain same fusion zone (ZF). Microstructures and microhardness results are compared to thermal measurements realized during the four welding. This study presents also a new way to characterize welding using infrared camera. It shows too an extension of the microhardness characterization, the mapping, made possible by using automated measurements.

## Experimental

6 mm (0.24 in.) thickness plates in 6061 T6 were used for this study. The MIG, pulsed MIG and CMT® MIG beads were realized with Fronius Transpuls Synergic 3200 CMT®. TIG bead was made with a Esseti Quad 450 AC/DC welding power supply. The filler wire used both for MIG and TIG was 5356 aluminum alloy of 1.2 mm (0.05 in.) of diameter.

Struers Durascan Vickers hardness tester was used to create a microhardness mapping from the weld bead and up to 25 mm (0.98 in.) in length. Thank to fully automatic measuring, about 1800 points, spaced of 300  $\mu\text{m}$  were performed, under a load of 0.1 kg.

The thermal measurements were realized using the infrared thermography. The camera is a FLIR Orion SC7500 equipped by an InSb sensor. A quasi-monochromatic filter of 3.35-3.45  $\mu\text{m}$  was used with two different integration times allowing to be sensitive from 175°C to 860°C (347°F to 1580°F). The acquisition frequency is 50Hz. The camera was placed in front of the plate. Figure 1 describes the experimental setup. Prior to measurements, plates were painted in black in order to work with a constant emissivity of 0.96.

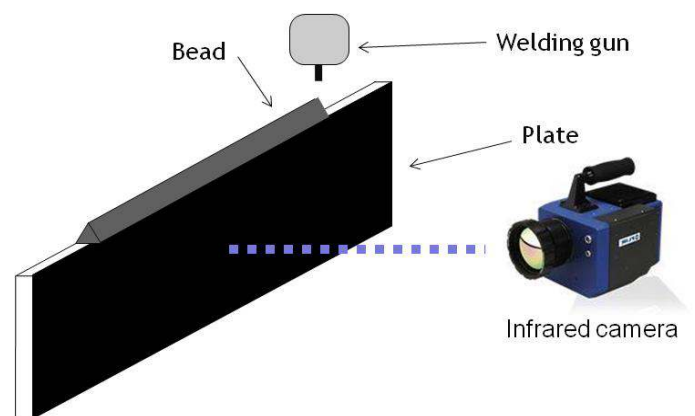


Figure 1: experimental setup of thermograph measurement

Transmission electron microscope used for this study was a FEI TECNAI G<sup>2</sup> 200kV. Transmission electron microscope

(TEM) examinations were done at the Institute of Metallurgy and Materials Science in Krakow (Poland). The thin foils were extracted from the HAZ using diamonded wire saw as showed in figure 2. Two samples were extracted in the HAZ of the MIG CMT® weld while the third was taken in the base metal. The zones were chosen in relation with the microhardness measurements. The final electropolishing was accomplished with Struers Tenupol-5 using commercial A2 electrolyte.

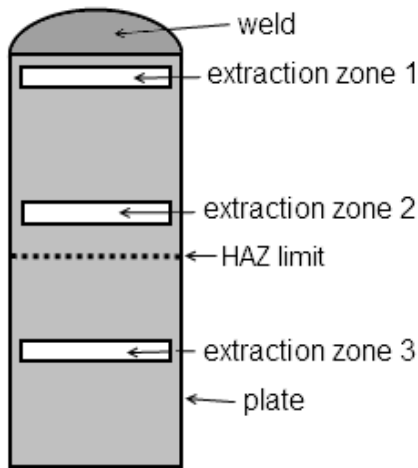


Figure 2: extraction zones in the plate

## Results

### 1- Infrared thermography

The temperature distribution under the bead was accurately measured by infrared thermography during the welding process. These measurements were performed at 1 mm (0.04 in.) under the weld toe, for all the processes. This non destructive and non invasive testing of the temperature allows saving thermal cycles of welding processes in real time. This information has great interest in welding processes and can be directly related to the microstructure and mechanical properties of weld joints. Indeed, the initial microstructure can be deeply affected by the welding heat. It is thus possible to predict the different types of precipitates formed as a function of the temperature reached, and this at any point of the welded plate metal.

According to thermograph in figure 3a, we found that thermal cycles of MIG and TIG are quite different. Indeed, for the same length of bead, the time of MIG welding are shorter than TIG welding. This is due to the characteristic of the TIG welding process with the feed rate can not exceed a few cm/min. Moreover, it is normal to observe very fast cooling rates for the three MIG processes. And as expected, the cooling rate of TIG process is longer. In addition, after 60 seconds, the arc breaking on the latter process leads to an acceleration of the cooling rate. This is represented by a change in slope on the thermograph curve.

Concerning the temperatures reached, for equivalent welding energies, MIG and pulsed MIG allow approaching 530°C (986°F), while the CMT® process achieved 640°C (1184°F) (figure 3b). This significant difference can affect the

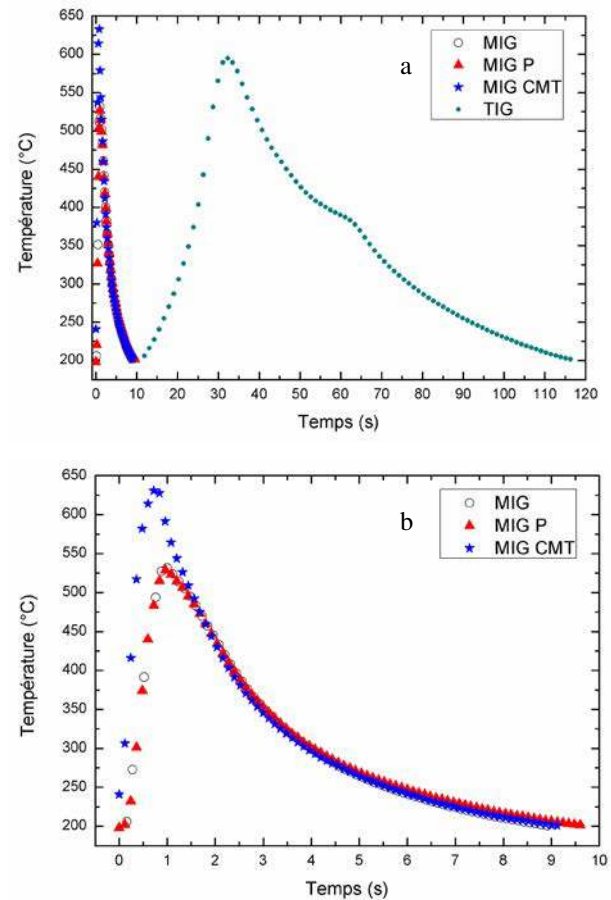


Figure 3: thermographs a) comparison of TIG and MIG processes, b) comparison of MIGs

microstructure with the formation of precipitates or the solution treatment of alloying elements.

With the TIG process, the peak temperature (maximal) reached during welding is higher than that achieved by the MIG “classic” process (close to 600°C – 1112°F).

### 2- Microhardness mapping

In order to evaluate the effects of the different thermal cycles on mechanical properties, microhardness mapping were performed on welded plate metal, from bead and on 25 mm (0.98 in.) in length and in cross-section (figure 4). The base metal, the aluminum alloy 6061-T6 has a hardness Vickers of 115, which corresponds to the blue color on the hardness scale.

First, the hardness gradients are parallel and normal to the surface. This means that the temperature of the surface of the plate is at point very close to that just below it.

Then, we see that the HAZ is very extensive with the TIG process since the hardness of the base metal is not recovered after 25 mm. The hardness is less than 80 HV, while with MIG processes the hardness of metal base is reached more quickly. The HAZ measures about 13 mm (0.51 in.) for MIG processes. This is explained by the low cooling rate of the TIG process, as observed in the thermograph (figure 3a). In the middle of the HAZ, the hardness varies between 50 and 70 HV (zone orange and red). These very low hardness values occur only with the TIG process. Further along in the HAZ, the hardness increases

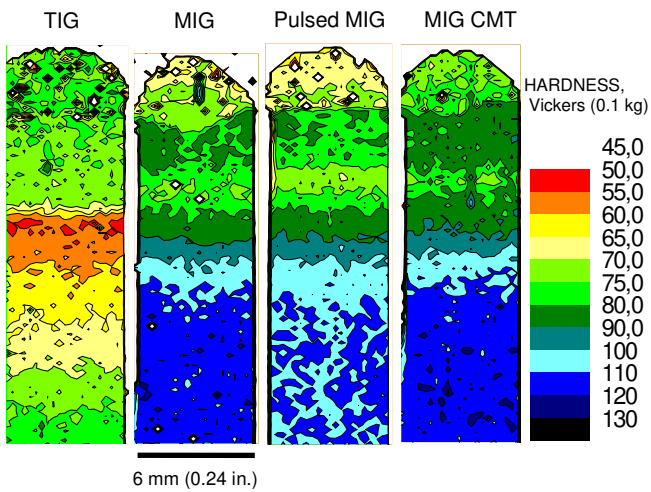


Figure 4: Hardness mapping HV0.1 of the four welding processes

slightly (dark and light yellow areas) but these values are still quite low. This can be explained considering the hardening precipitation of the 6061 aluminum alloy [12]. The strengthening precipitates  $\beta''$  present at T6 state are metastable and evolve spontaneously with temperature raising. So,  $\beta''$  changes into  $\beta'$  phase and finally into the  $\beta$  phase which is stable [9]. However the strengthening ability of these precipitates is low. This induces a decreasing of the mechanical properties and therefore a decrease of hardness. It is therefore very likely that in the yellow and orange-red areas, we can observe this transformation sequence of metastable phases, including the presence of precipitates  $\beta'$  in large amount. Then these precipitates probably change partially into  $\beta$  phase, in the red-orange area. The well-defined hardness gradient in several layers is so easily explained by the transformation of  $\beta''$ , by the coexistence of one or more phases and by their density.

Finally, the hardness increases again in the beginning of the HAZ, near the molten zone. This can be explained by a partial reversion of the precipitates because the temperature reached exceeds  $530^{\circ}\text{C}$  ( $986^{\circ}\text{F}$ ) with this process. And, this temperature corresponds to the equilibrium solid solubility limit of the 6061 alloy, according to the pseudo-binary diagram Al-Mg<sub>2</sub>Si. Thus, the dissolution of precipitates leads

to a release of alloying elements (Mg and Si) into the aluminum matrix. So this solutioning of  $\beta'$  and  $\beta$  particles produces a supersaturated solid solution  $\alpha'$ . And by aging, the hardness slightly increases until a moderate stage [9].

The evolution of the hardness of the three MIG processes is very similar between them, with some details yet. The extent of the HAZ is about 13 mm (0.51 in.) for all the three cases and the average hardness levels are similar. Indeed, in all cases, the hardness is greater than the hardness obtained by the TIG process. Arguably, we can state that, for similar welds in form, the TIG process further deteriorates mechanical properties of weld joints, with an extremely extended HAZ and lower hardness. With the pulsed MIG process, it seems that the hardness is less homogeneous in the different layers, especially approaching the base metal (mixed light and dark blue). So the size of the HAZ is maybe larger. Others measurements are needed to be sure.

Regarding the CMT® process, it is interesting to note that in the HAZ near the molten zone, the hardness is generally higher than for the two other MIG processes. This difference can be explained by a higher temperature reached during welding. Indeed, as noted above, the MIG CMT® process allows rising  $640^{\circ}\text{C}$  ( $1184^{\circ}\text{F}$ ). Thus, as with the TIG process, a partial solutioning is possible, and the dissolved precipitates release alloying elements to produce a supersaturated solid solution. With these hardness values obtained (between 80 and 90 HV – dark green area), this area can be considered as T4 temper state.

### 3 - TEM results

To confirm the results of hardness as well as hypothesis made above, electron microscopy in transmission was undertaken on the alloy welded by Cold Metal Transfer (figure 5).

The bright field image figure 5a corresponds to an extracted zone in the base metal. The needles shape of the precipitates and their size suggest that this is the  $\beta''$  metastable phase, normally observed in the Al-Mg-Si alloys, in the T6 state. Various publications [13, 14] of the study of  $\beta''$  phase describe its particles as needles directed along the three axes  $\langle 001 \rangle_{\text{Al}}$ . These fine needles about 50 nm in length also appear as dark spots pointing in the viewing direction, with an average diameter of 4 nm. Thanks to the presence of such precipitates, it is possible to achieve the maximum hardness values. According to [13], the maximum hardness is achieved when the alloy contains a combination of very fine Guinier-

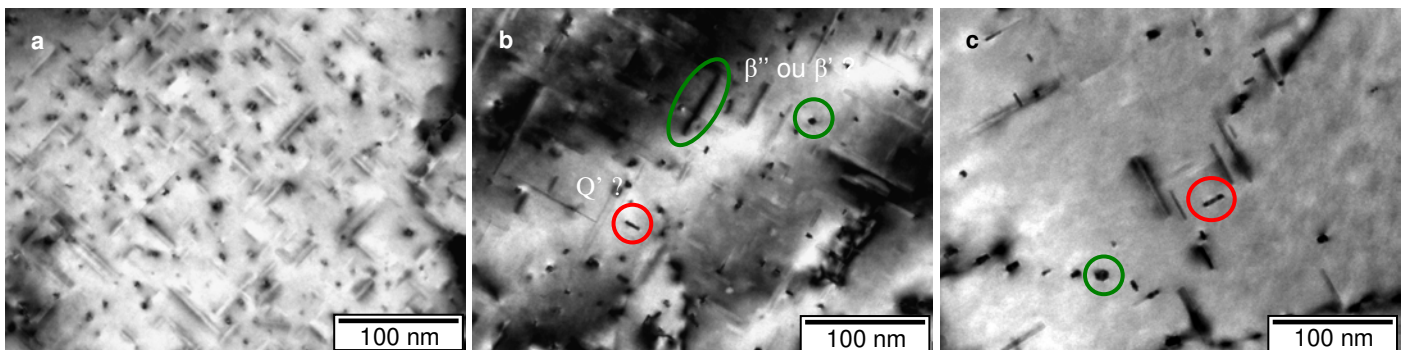


Figure 5: TEM images extracted of MIG CMT process – a) in metal base, b) at the beginning of the HAZ (area corresponding to 90-100 HV, c) in the HAZ near the molten zone (corresponding to 75-90 HV)

Preston zones (GP-1) and larger needles  $\beta''$  phase, with a number density in the matrix of about  $10^4/\mu\text{m}^3$ .

The bright field image figure 5b corresponds to an extracted zone in the HAZ near the base metal. The density of precipitates seems to be lower in this area than in the base metal.  $\beta''$  phase is always present. However, its changes of morphology in some places (green circles). It appears coarser. Therefore, it could be also the  $\beta'$  phase. Indeed, according to Dumolt [15] increasing the aging temperature leads to a softening of the alloy due to coarsening of  $\beta''$  precipitates. Because of the nanometric size of these particles, it is difficult to distinguish them. High resolution microscopy (TEM/HREM) or atom-probe field-ion microscopy (APFIM) investigations for example, would help to have more specific evidences [16]. This has not been done in this study. However, the presence of a new phase (red circle) in laths shape can be observed. According to [17], it could be the  $Q'$  phase, metastable phase in the ternary alloys Al-Mg-Si where silicon content is in excess, the  $Q'$  phase equilibrium in the quaternary system Al-Mg-Si-Cu alloys. Both phenomena ( $\beta''$  transformation and presence of a new phase) contribute to a slightly but significant softening of the alloy.

The bright field image figure 5c corresponds to an extracted zone in the HAZ near the molten zone. The density of precipitates decreases again. The  $\beta''$  no longer seems to be present. The  $\beta''$  fade-out, combined with the presence of precipitates coarser and therefore fewer, lead to a high decrease of hardness. This microstructure, with a very low density of precipitates is consistent with the hypothesis of partial dissolution during the welding.

## Conclusions

In this study we tried to correlate the physical parameters (temperatures, thermal cycles) associated with the four welding processes (MIG, pulsed MIG, MIG CMT®, and TIG) with mechanical properties (hardness) and microstructure (TEM study of precipitates). This study only focused on the HAZ zones of the 6061-T6 alloy.

Thermography provides an accurate estimation of the temperature reached during welding, as well as the heating and cooling rate. With the MIG CMT®: "Cold Metal Transfer" the temperature reached is higher than those obtained with MIG and pulsed MIG, for same welding linear energies. This is quite surprising, considering the name given of this process. However, this process provides the best results of hardness. Indeed, the size of the HAZ is identical to those of the two others MIG processes. But the average hardness, in particular near the weld bead, is higher.

Comparative hardness tests (conducted from the bead and up to 25 mm in length) carried out by mapping is a new visual way to present the evolution of mechanical properties.

Finally, with an initial TEM study, it was possible to establish a direct relationship between the evolution of hardness and the presence of different precipitates.

Among the outlook, high resolution TEM studies could allow to have more precise identifications of the different precipitates. Calorimetric measurements are also planned to

identify the sequence of different phase transformations, and to know at which temperatures these transformations occur.

## Acknowledgments

The authors would like to greatly acknowledge Lidia Lityńska-Dobrzyńska for TEM examinations.

## References

- [1] Parson NC, Yiu HL. Light metals 1989 Campbell PG, editor. PA, USA, Warrendale TMS; (1989), pp. 713–24.
- [2] Buha J., Lumley R.N. and Crosky A.G. "Microstructural Development and Mechanical Properties of Interrupted Aged Al-Mg-Si-Cu Alloy" *Metallurgical And Materials Transactions A* Vol. 37A, (2006), pp. 3119-3130
- [3] Ozturk F., Sisman A., Toros S., Kilic S., Picu R.C. "Influence of aging treatment on mechanical properties of 6061 aluminum alloy" *Materials and Design* Vol. 31 (2010) pp. 972–975
- [4] Dutta I., Allen S.M. "A calorimetric study of precipitation in commercial aluminium alloy 6061" *Journal Of Materials Science Letters* Vol.10, (1991), pp.323-326
- [5] Cieslak M.J. and Fuerschbach P. W. "On the Weldability, Composition, and Hardness of Pulsed and Continuous Nd:YAG Laser Welds in Aluminum Alloys 6061,5456 and 5086" *Metallurgical Transactions B* Vol. 19B, (1988), pp.319-329.
- [6] Hirose A., Todaka H., Yamaoka H., Kurosawa N. and Kobayashi K.F., "Quantitative Evaluation of Softened Regions in Weld Heat-Affected Zones of 6061-T6 Aluminum Alloy—Characterizing of the Laser Beam Welding Process" *Metallurgical And Materials Transactions A* Vol. 30A, (1999) pp.2115-2120.
- [7] Moreira P. M. G. P., Richter-Trummer V. and de Castro P. M. S. T. "Fatigue Behaviour of FS, LB and MIG Welds of AA6061-T6 and AA6082-T6" *Multiscale Fatigue Crack Initiation and Propagation of Engineering Materials: Structural Integrity and Microstructural Worthiness* G.C. Sih (ed.) (2008) pp.85-111
- [8] Ahmad R., Bakar M.A. "Effect of a post-weld heat treatment on the mechanical and microstructure properties of AA6061 joints welded by the gas metal arc welding cold metal transfer method " *Materials and Design*, Vol.32, (2011), 5120–5126.
- [9] Malin V. "Study of Metallurgical Phenomena in the HAZ of 6061-T6 Aluminum Welded Joints" *Welding Research Supplement I* (1995) pp. 305-318.
- [10] Murr L. E., Liu G., McClure J. C., "A TEM study of precipitation and related microstructures in friction-stir-welded 6061 aluminium" *Journal Of Materials Science* Vol. 33, (1998) , pp. 1243 — 1251
- [11] Woo W., Choo H., Withers P. J., Feng Z. "Prediction of hardness minimum locations during natural aging in an aluminum alloy 6061-T6 friction stir weld" *J Mater Sci*, Vol. 44, (2009), pp.6302–6309.
- [12] Edwards G. A., Stiller K., Dunlop G. L. and Couper M. J. "The Precipitation Sequence in Al–Mg–Si Alloys" *Acta mater.* Vol. 46, No. 11,(1998), pp. 3893–3904



- [13] Andersen S. J., Zandbergen H. W., Jansen J., Træholt C., Tundal U. and Reiso O. "The Crystal Structure of the  $\beta$ ' Phase in Al-Mg-Si Alloys" *Acta mater.* Vol. 46, No. 9, (1998), pp. 3283–3298
- [14] Yao J.Y., Graham D.A., Rinderer B., Couper M.J. "A TEM study of precipitation in Al-Mg-Si alloys", *Micron*, Vol.32, (2001), pp.865-870
- [15] Dumolt S.D., Laughlin D.E. and Williams J.C. "Formation of a Modified  $\beta$ ' Phase in Aluminium Alloy 6061" *Scripta Metallurgica* Vol.18, (1984), pp.1347-1350.
- [16] Hasting H.K., Lefebvre W., Marioara C., Walmsley J.C., Andersen S., Holmestad R. and Danoix F. "Comparative study of the  $\beta$ ' phase in a 6xxx Al alloy by 3DAP and HRTEM" *Surf. Interface Anal.* Vol. 39, (2007), pp.189–194
- [17] Chakrabarti D.J., Laughlin D. E. "Phase relations and precipitation in Al-Mg-Si alloys with Cu additions" *Progress in Materials Science* Vol.49, (2004), pp. 389–410